Tetranuclear Polypyridyl Complexes of Ru^{II} and Fe^{II}: Synthesis, Electrochemical, Photophysical and Photochemical Behaviour

Jean Lombard,[a] Sophie Romain,[a] Stéphane Dumas,[a] Jérôme Chauvin,[a] Marie-Noëlle Collomb,[a] Denis Daveloose,[b] Alain Deronzier,*[a] and Jean-Claude Leprêtre*[a]

Keywords: Bridging ligands / Electrochemistry / Iron / Photochemistry / Ruthenium

Three heterotetranuclear complexes $[\{Ru^{II}(bpy)_2(LL_n)\}_3Fe^{II}]^{8+}$ {bpy = 2,2′-bipyridine, n = 2, 4, 6; denoted $[\{Ru(LL_n)\}_3Fe]^{8+}$}, in which one iron centre is complexed by three Ru^{II}-tris-bipyridine-like moieties containing covalently bridging bis-bipyridine LL_n ligands, have been synthesised and characterised. The stability and the electrochemical, photophysical and photochemical properties of these complexes have been investigated in CH_3CN. The cyclic voltammograms of all complexes exhibit two successive reversible oxidation processes in the positive region, corresponding to the Fe^{II}/Fe^{III} and Ru^{II}/Ru^{III} redox couples. These systems are clearly separated ($\Delta E_{1/2}$ about 300 mV), which indicates the absence of an electronic connection between the two subunits. In the negative region, three successive reversible four-electron systems are observed, corresponding to the ligand-based reduction processes. The two oxidized forms of the complexes $[\{Ru^{II}(LL_n)\}_3Fe^{III}]^{9+}$ and $[\{Ru^{III}(LL_n)\}_3Fe^{III}]^{12+}$, which are obtained by two successive exhaustive electrolyses, are very stable. The $[\{Ru(LL_n)\}_3Fe]^{8+}$ complexes are luminescent, which shows that the covalent linkage between the Ru^{II}-tris-bipyridine and Fe^{II}-tris-bipyridine subunits leads to an only partial quenching of the Ru^{II*} excited states by energy transfer to the Fe^{II} centre. The luminescence lifetime and quantum yield are found to be independent of the complexes′ concentration, thus indicating that the energy-transfer process is only due to an intramolecular electron-exchange mechanism. Quantitative photoinduced oxidation of the tetranuclear complexes has been performed by continuous photolysis experiments in the presence of a large excess of a diazonium salt, which plays the role of a sacrificial oxidant. Two successive oxidation processes ($Fe^{II} \rightarrow Fe^{III}$ and $Ru^{II} \rightarrow Ru^{III}$) are observed.

Introduction

In recent years, important synthetic efforts have been made to mimic the function of the donor site of the photosystem II (PSII) by the development of superstructured heterometallic complexes.[1–3] The main strategy to elaborate models of PSII involves the covalent coupling of a photoactive $[Ru^{II}(bpy)_3]^{2+}$ (bpy = 2,2′-bipyridine) moiety, which plays the role of the P_{680} chlorophyll photosensitizer, to some monomanganese(II), binuclear (II,III) or (III,III) and trinuclear (II,II,II) complexes that model the catalytic centre that oxidizes water into oxygen.[4–7] It has been reported for the mononuclear manganese(II) complexes that an intramolecular electron transfer can occur from the Mn^{II} site to the photogenerated Ru^{III} species in the presence of an external electron acceptor like viologen in acetonitrile.[8] However, the rate constant for this process is fairly slow and the efficiency of the process depends on the distance between the two metallic centres. In addition, the system is complicated, since the Mn^{II}/Mn^{III} redox couple is only poorly reversible as the Mn^{III} species reacts with residual water to form binuclear Mn^{III}/Mn^{IV} oxo complexes.[9–11] Moreover, in most cases the Mn^{II} sites quench the excited state of the ruthenium(II) complex, presumably by an energy-transfer process.[8,12,13] With a view to studying this kind of intramolecular electron transfer, we have recently reported the photoredox behaviour of a series of heterobinuclear metallic complexes of Ru^{II} and Fe^{II}, namely $[Ru^{II}(bpy)_2(LL_n)\text{-}Fe^{II}(bpy)_2]^{4+}$ (denoted $[Ru(LL_n)Fe]^{4+}$), based on the use of bridging bis-bipyridine ligands LL_n (Scheme 1).[14] This system is simpler than the Ru^{II}/Mn^{II} one, since Fe^{II}/Fe^{III} is a perfectly reversible redox couple, with the oxidation of the $[Fe^{II}(bpy)_3]^{2+}$-like complex occurring at a potential close to that of $[Mn^{II}(bpy)_3]^{2+}$. In this previous study, we demonstrated that the ^{3}MLCT excited state of the Ru^{II}-tris-bipyridine centre is strongly quenched by the Fe^{II}-tris-bipyridine

[a] Laboratoire d′Electrochimie Organique et de Photochimie Rédox, Université Joseph Fourier,
UMR CNRS 5630, Institut de Chimie Moléculaire de Grenoble, FR CNRS 2607
B. P. 53, 38041 Grenoble Cedex 9, France
Fax: +33-4-7651-4267
E-mail: jean-claude.lepretre@ujf-grenoble.fr
alain.deronzier@ujf-grenoble.fr
[b] Centre de Recherches du Service de Santé des Armées "Emile Pardé", Laboratoire de Biospectrométrie,
24 Avenue des Maquis du Grésivaudan, BP 87, 38702 La Tronche, Cedex, France

  DOI: 10.1002/ejic.200500106

unit through an energy-transfer process that is mainly intermolecular. Nevertheless, this strong energy transfer can be easily short-circuited in the presence of an external irreversible electron acceptor like an aryldiazonium salt (ArN_2^+) by an electron transfer that leads finally to the photoinduced formation of $[Ru^{II}(LL_n)Fe^{III}]^{5+}$ species with high efficiency. It has been shown that the electron transfer between the ground state of the Ru^{III} and Fe^{II} species essentially occurs by an intermolecular process. In order to gain more information about these photoprocesses, we have synthesised a series of new heterobimetallic complexes of Ru^{II} and Fe^{II}: $[\{Ru^{II}(bpy)_2(LL_n)\}_3Fe^{II}]^{8+}$ {n = 2, 4, 6; denoted $[\{Ru(LL_n)\}_3Fe]^{8+}$} in which one iron centre is complexed by three Ru^{II}-tris-bipyridine moieties (Scheme 1). A previous publication reported some photophysical data of this kind of complex, but these compounds were only prepared in situ.[15] Under these conditions, the presence of some uncomplexed $[Ru^{II}(bpy)_2(LL_n)]^{2+}$ {denoted $[Ru^{II}(LL_n)]^{2+}$} species in the medium prevented the drawing of clear conclusions about the photophysical properties of the $[\{Ru(LL_n)\}_3Fe]^{8+}$ complexes. In the present study, we report the synthesis and characterisation of the three heterotetranuclear complexes $[\{Ru(LL_n)\}_3Fe]^{8+}$, their main redox and photophysical properties and the comparison of the latter properties with those of the heterobinuclear complexes $[Ru(LL_n)Fe]^{4+}$. Moreover, we have investigated the possibility to photoinduce the oxidation of the tetranuclear complexes in the presence of ArN_2^+. The expected multi-step oxidation process is summarised in Scheme 2.

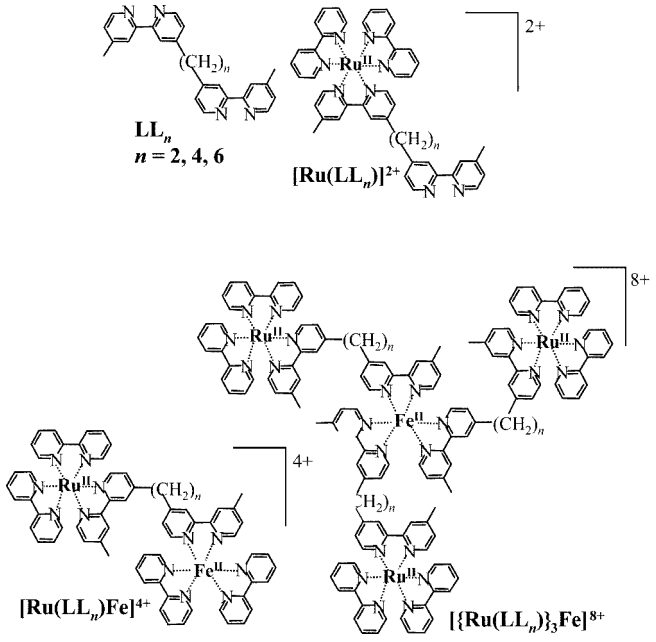

Scheme 1. Chemical structure of the ligands LL_n and of the complexes $[Ru(LL_n)]^{2+}$, $[Ru(LL_n)Fe]^{4+}$ and $[\{Ru(LL_n)\}_3Fe]^{8+}$.

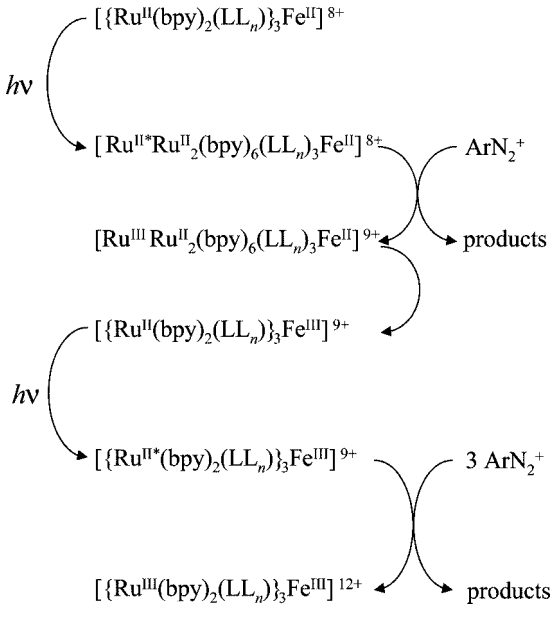

Scheme 2. Schematic presentation of the photooxidation mechanism of $[\{Ru(LL_n)\}_3Fe]^{8+}$ in the presence of an external electron acceptor (ArN_2^+).

Results and Discussion

Synthesis and Stability of the Complexes

Eliott and co-workers[15] have reported that the complexation of some $[Ru^{II}(bpy)_2(L\text{-}L)]^{2+}$ complexes (L-L = covalently linked bipyridines) with Fe^{2+} in situ in methanol/water (1:1) forms the tetranuclear complexes $[\{Ru^{II}(bpy)_2(L\text{-}L)\}_3Fe^{II}]^{8+}$. However, in this medium, it has been shown that such compounds undergo some dissociation (association constants between 10^{13} and 10^{15}). As a result, the presence of uncomplexed $[Ru^{II}(bpy)_2(L\text{-}L)]^{2+}$ species leads to the observance of a double exponential for the emission decay. The fast component of the decay corresponds to emission from ruthenium "ligands" complexed to iron, and the long one to the uncomplexed $[Ru^{II}(bpy)_2(L\text{-}L)]^{2+}$ centres. Moreover, isolation of tetranuclear complexes in a pure form by this group was unsuccessful. In this work, we have synthesised, isolated and purified three heterotetranuclear complexes $[\{Ru(LL_n)\}_3Fe]^{8+}$ (n = 2, 4 and 6) by the treatment of 0.4 equivalents of Fe^{2+}, as its perchlorate salt, with one equivalent of the corresponding $[Ru(bpy)_2(LL_n)]^{2+}$ complexes in ethanol/water (12:1). This synthetic method allows us to obtain the expected compounds with fairly good yields; their purity was checked by TLC and elemental analysis. In order to determine their photophysical properties in CH_3CN solution properly, we also verified their stability in this solvent by UV/Vis spectroscopy. The visible absorption spectra of $[\{Ru(LL_n)\}_3Fe]^{8+}$ in the concentration range 10^{-4}–10^{-7} M exhibit the expected regular bands at 356, 396 (shoulder), 430 (shoulder), 454 and 530 nm (shoulder) corresponding to the superimposition of the absorbance of the Ru^{II}- and Fe^{II}-tris-bipyridine subunits (Table 1).[15] For the three complexes $[\{Ru(LL_n)\}_3Fe]^{8+}$, there is no significant variation of the ratio of the absorbance values at 356, 454 and 530 nm with concentration (in the range 10^{-4} and 10^{-7} M), showing that no dissociation of the complexes occurs. The linearity of the absorbance vs.

Table 1. UV/Vis data for $[Ru^{II}(LL_n)]^{2+}$ and $[\{Ru^{II}(LL_n)\}_3Fe^{II}]^{8+}$ in deoxygenated CH_3CN + 0.1 M Bu_4NClO_4 at 25 °C.

Complexes	λ_{abs} (ε)	Ref.
$[Fe^{II}(dmbpy)_3]^{2+}$	356 nm (7100 $M^{-1}cm^{-1}$), 395[a] (4000) 494[a] (7400), 528 (8000)	this work
$[Fe^{III}(dmbpy)_3]^{3+}$	417 (2200)	this work
$[Ru^{II}(LL_2)]^{2+}$	354[a] (5500), 396[a] (5100) 430[a] (10300), 454 (12000)	[14]
$[Ru^{II}(LL_4)]^{2+}$	354[a] (5500), 396[a] (5200) 430[a] (10700), 454 (12300)	[14]
$[Ru^{II}(LL_6)]^{2+}$	354[a] (5700), 396[a] (5400) 430[a] (11000), 454 (12700), 356[a] (25000)	[14]
$[\{Ru^{II}(LL_2)\}_3Fe^{II}]^{8+}$	396[a] (20500), 430[a] (35000) 455 (40900), 530[a] (9300)	this work
$[\{Ru^{II}(LL_4)\}_3Fe^{II}]^{8+}$	356[a] (26000), 396[a] (21400), 430[a] (36600) 454 (42500), 530[a] (11800)	this work
$[\{Ru^{II}(LL_6)\}_3Fe^{II}]^{8+}$	356[a] (27300), 396[a] (22200), 430[a] (36600) 454 (42300), 530[a] (12700)	this work

[a] Shoulder.

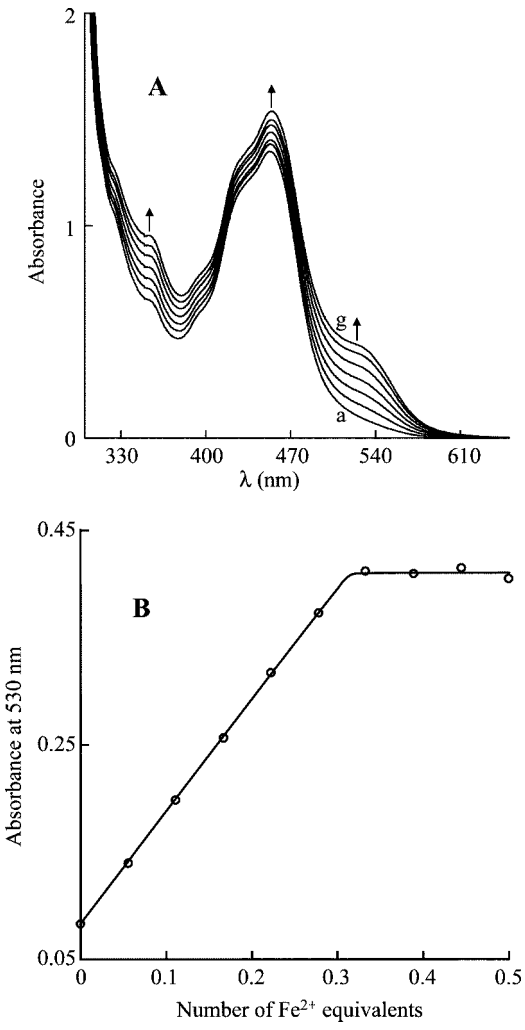

Figure 1. A) Evolution of the visible spectrum of a solution of $[Ru(LL_4)]^{2+}$ (0.105 mM) in CH_3CN + 0.1 M Bu_4NClO_4 during the addition of $Fe(ClO_4)_2 \cdot 8H_2O$: a) initial solution, b) after addition of 0.055 equiv. of Fe^{2+}, (c) 0.11, (d) 0.167, (e) 0.22, (f) 0.28, (g) 0.33 and 0.5. B) Evolution of the absorbance at 530 nm (l = 1 cm).

addition of Fe^{2+} allows the determination of the association constant as being greater than 10^{22}. This constant value is higher than those estimated in a methanol/water mixture (10^{13}–10^{15}),[15] presumably due to the more dissociative properties of this medium compared to the acetonitrile one. This high stability was also confirmed by following the absorbance at 530 nm of a $[Ru(LL_n)]^{2+}$ acetonitrile solution after progressive addition of $Fe(ClO_4)_2 \cdot 8H_2O$ (Figure 1). The absorbances at 356 and 530 nm increase linearly during the addition of Fe^{2+} until a maximum is reached for the expected ratio of one iron for every three $[Ru(LL_n)]^{2+}$ units. Addition of an excess of Fe^{2+} does not lead to any spectroscopic changes. The absence of free $[Ru(LL_n)]^{2+}$ is also confirmed by luminescence measurements in CH_3CN, since, for all synthesised complexes, the emission decay curves are clean single exponentials (see below).

Electrochemistry

In CH_3CN containing 0.1 M Bu_4NClO_4 the electrochemical behaviour of the three $[\{Ru(LL_n)\}_3Fe]^{8+}$ complexes is similar (see Table 2). The length of the aliphatic bridges has only a slight effect on the $E_{1/2}$ values of the oxidative and reductive processes. In the negative region, although the successive one-electron reductions of the bipyridine ligands in the $[Fe(dmbpy)_3]^{2+}$ (dmbpy = 4,4′-dimethyl-2,2′-bipyridine) and $[Ru(LL_n)]^{2+}$ complexes are clearly separated (by 115–140 mV, see Table 2), the reduction pattern of the $[\{Ru(LL_n)\}_3Fe]^{8+}$ complexes shows only three successive reduction waves {see Figure 2 for $[\{Ru(LL_4)\}_3Fe]^{8+}$}, as observed previously for the binuclear $[Ru(LL_n)Fe]^{4+}$ complexes.[14] Moreover, only the first reduction wave is clearly seen. A strong adsorption phenomenon coupled to the second reduction process leads to an important distortion of the third one. It should be mentioned that each reversible redox system corresponds to the overall exchange of four electrons corresponding to the one-electron reduction of one bipyridine unit per metallic centre. The exchange of

Table 2. Electrochemical data for $[Ru^{II}(bpy)_2(LL_n)]^{2+}$ and $[\{Ru^{II}(LL_n)\}_3Fe^{II}]^{8+}$ in deoxygenated CH_3CN + 0.1 M Bu_4NClO_4 using a platinum electrode at a scan rate of 100 mV s^{-1}.[a]

Complexes	Fe^{II}/Fe^{III}	Ru^{II}/Ru^{III}	Reduction processes 1	2	3	Ref.
$[Fe^{II}(dmbpy)_3]^{2+}$	0.585 (60)	–	–1.775 (60)	–1.970 (70)	–2.195 (70)	this work
$[Ru^{II}(LL_2)]^{2+}$	–	0.912 (60)	–1.665 (50)	–1.855 (50)	–2.105 (50)	[14]
$[Ru^{II}(LL_4)]^{2+}$	–	0.905 (60)	–1.665 (50)	–1,862 (50)	–2.115 (50)	[14]
$[Ru^{II}(LL_6)]^{2+}$	–	0.905 (60)	–1.665 (50)	–1.865 (50)	–2.125 (50)	[14]
$[\{Ru^{II}(LL_2)\}_3Fe^{II}]^{8+}$	0.607 (60)	0.907 (60)	–1.687 (60)	–1.827 (80)	[b]	this work
$[\{Ru^{II}(LL_4)\}_3Fe^{II}]^{8+}$	0.588 (60)	0.905 (60)	–1.647 (70)	–1.806 (50)	[b]	this work
$[\{Ru^{II}(LL_6)\}_3Fe^{II}]^{8+}$	0.588 (60)	0.902 (60)	–1.658 (60)	–1.818 (70)	[b]	this work

[a] $E_{1/2}$ (V) (ΔEp in mV) vs. Ag/Ag^+ (0.01 M $AgNO_3$ in CH_3CN + 0.1 M Bu_4NClO_4). [b] This value cannot be accurately measured since the waves are strongly distorted by adsorption phenomena (see text).

four electrons is confirmed by the fact that the height of the first reduction wave at a rotating disk electrode is equal to the sum of the heights of the two oxidation waves (see below and Figure 2).

In the positive region, the cyclic voltammograms of the three $[\{Ru(LL_n)\}_3Fe]^{8+}$ complexes exhibit two well-separated reversible redox systems (Figure 2). The potentials of these systems are closed to those of the mononuclear complexes $[Fe(dmbpy)_3]^{2+}$ and $[Ru(LL_n)]^{2+}$, thus allowing us to assign the first oxidative process to the Fe^{II}/Fe^{III} redox couple and the more anodic one to that of the Ru^{II}/Ru^{III} system (Table 2). Moreover, rotating disk electrode experiments confirmed that the complexes are obtained in pure form and that no dissociation occurs in CH_3CN, since the height of the Ru^{II}/Ru^{III} wave is three times that of Fe^{II}/Fe^{III}, in accordance with the 3:1 Ru/Fe stoichiometry in the tetranuclear complexes [Equations (1) and (2)].

$$[\{Ru^{II}(bpy)_2(LL_n)\}_3Fe^{II}]^{8+} \rightarrow [\{Ru^{II}(bpy)_2(LL_n)\}_3Fe^{III}]^{9+} + e^- \quad (1)$$

$$[\{Ru^{II}(bpy)_2(LL_n)\}_3Fe^{III}]^{9+} \rightarrow [\{Ru^{III}(bpy)_2(LL_n)\}_3Fe^{III}]^{12+} + 3e^- \quad (2)$$

As previously observed for the $[Ru(LL_n)Fe]^{4+}$ complexes,[14] the $E_{1/2}$ values of the Fe^{II}/Fe^{III} and Ru^{II}/Ru^{III} redox systems decrease slightly upon increasing the number of methylenes in the aliphatic bridge (Table 2). This $E_{1/2}$ variation is due to a slightly higher electron-donor effect of the LL_6 ligand compared to LL_4, and of the latter to LL_2.

Otherwise, the Ru^{II}/Ru^{III} redox system involves the simultaneous exchange of three electrons. In order to estimate the magnitude of the electronic connexion between the three ruthenium centres, computational fitting of the cyclic voltammetry curves of $[\{Ru(LL_n)\}_3Fe]^{8+}$ was performed, which led to the determination of the formal potentials E_f^1, E_f^2 and E_f^3 for the three ruthenium oxidation steps (Table 3) (see Figure 3 for $[\{Ru(LL_4)\}_3Fe]^{8+}$ and Experimental Section).[16,17] Since the difference between the extreme E_f values ($\Delta E_f^{3-1} = E_f^3 - E_f^1$) is close to the theoretical value (57 mV) for the three tetranuclear complexes,[16] the absence of an electronic connexion within the studied compounds is confirmed. One can see, as observed for the Fe^{II}/Fe^{III} system, that these E_f values are in accordance with the electron-donor character of the bridging ligand; the $E_{1/2}$ value of the Ru^{II}/Ru^{III} couple decreases slightly

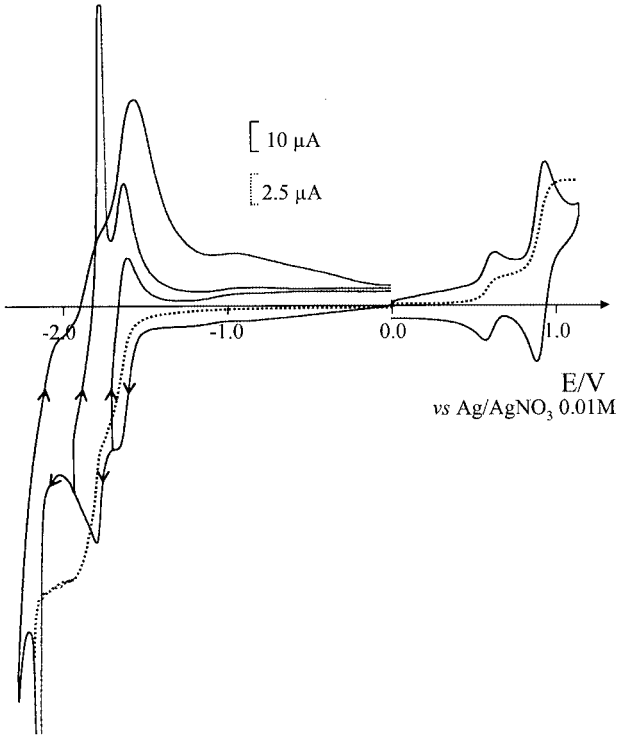

Figure 2. (–) Cyclic voltammograms of a 0.32 mM solution of $[\{Ru(LL_4)\}_3Fe]^{8+}$ in CH_3CN + 0.1 M Bu_4NClO_4 at a platinum electrode; scan rate: 100 mV s^{-1}. (---) Voltammograms at a platinum rotating disk electrode at ω = 600 r min^{-1}; scan rate: 10 mV s^{-1}.

(10 mV) in the order $LL_2 > LL_4 > LL_6$. Since the two oxidized forms of the complexes, $[\{Ru^{II}(LL_n)\}_3Fe^{III}]^{9+}$ and $[\{Ru^{III}(LL_n)\}_3Fe^{III}]^{12+}$ are expected to be produced during the photoinduced electron-transfer processes (Scheme 2), the stabilities of these species were evaluated by exhaustive electrolyses. Taking into account the large potential difference between the Fe^{II}/Fe^{III} and Ru^{II}/Ru^{III} redox systems ($\Delta E_{1/2}$ = 296 mV for LL_2, 315 for LL_4 and 317 for LL_6), the mixed-valent $[\{Ru^{II}(LL_n)\}_3Fe^{III}]^{9+}$ species are perfectly stable. Indeed, two successive exhaustive electrolyses carried out at 0.80 and 1.10 V consumed one and three electrons, respectively, per $[\{Ru(LL_n)\}_3Fe]^{8+}$, and allowed the bulk build-up of $[\{Ru^{II}(LL_n)\}_3Fe^{III}]^{9+}$ and $[\{Ru^{III}(LL_n)\}_3Fe^{III}]^{12+}$. This is illustrated by the evolution of the absorption spectra of the solutions after these sequential electrolyses

Table 3. Oxidation potentials of $[\{Ru(LL_n)\}_3Fe]^{8+}$ determined by fitting of the experimental cyclic voltammograms.

	$E_{1/2}$ [mV] vs. Ag/Ag^+ 10 mM				
Complexes	Fe^{II}/Fe^{III} $E_{1/2}$	Ru^{II}/Ru^{III} E_f^1	Ru^{II}/Ru^{III} E_f^2	Ru^{II}/Ru^{III} E_f^3	Ru^{II}/Ru^{III} $E_{1/2}^{moy}$ (ΔE_f^{3-1})
$[\{Ru^{II}(LL_2)\}_3Fe^{II}]^{8+}$	614	882 ± 1	915 ± 2	934 ± 3	910 (58)
$[\{Ru^{II}(LL_4)\}_3Fe^{II}]^{8+}$	584	860 ± 2	906 ± 2	931 ± 2	899 (71)
$[\{Ru^{II}(LL_6)\}_3Fe^{II}]^{8+}$	572	852 ± 1	897 ± 4	818 ± 10	889 (66)

(see Figure 4 for LL_4). The typical initial bands of the Fe^{II}-tris-bipyridine unit (λ = 356 and 530 nm) disappear after one electron per complex has been passed (Table 1). After exchange of three other electrons, the bands of the Ru^{II}-tris-bipyridine units (λ = 356 and 454 nm) disappear and are replaced by those of the Ru^{III} ones (428 and 644 nm). Both oxidized forms are stable for several hours. Finally, we found that exhaustive reduction of all these oxidized species leads to the nearly quantitative recovery of the starting material, thus demonstrating the high reversibility of the process.

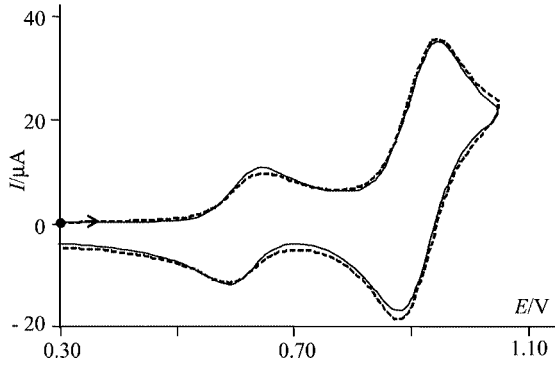

Figure 3. Cyclic voltammograms of a 0.14 mM solution of $[\{Ru(LL_4)\}_3Fe]^{8+}$ in CH_3CN + 0.1 M Bu_4NClO_4 at a platinum electrode; scan rate 200 mV s^{-1}: (---) experimental curve, (−) fitted curve.

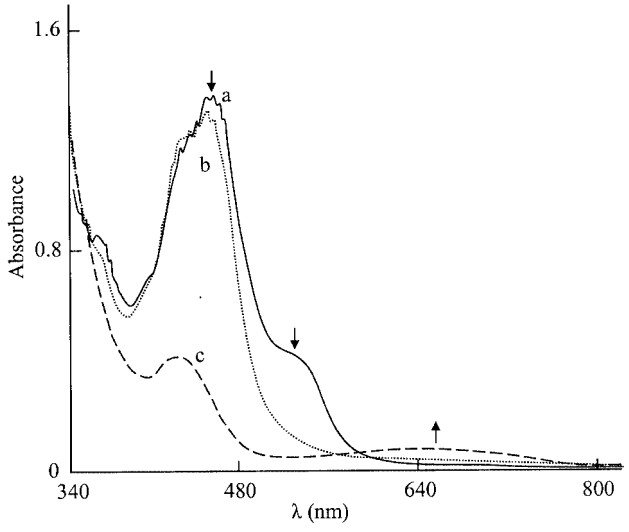

Figure 4. Absorption spectra of a 0.32 mM solution of $[\{Ru(LL_4)\}_3Fe]^{8+}$ in CH_3CN + 0.1 M Bu_4NClO_4: (a) initial solution, (b) after exhaustive electrolysis at 0.80 V, (c) after exhaustive electrolysis at 1.10 V (l = 1 mm).

Energy Transfer

The emission wavelength (λ_{emis}), luminescence lifetime (τ), and luminescence quantum yield (φ_L) of the $[\{Ru(LL_n)\}_3Fe]^{8+}$ complexes are reported in Table 4, along with those obtained for the corresponding $[Ru(LL_n)]^{2+}$ and $[Ru(LL_n)Fe]^{4+}$ parent complexes. On the nanosecond timescale, the luminescence decay of all $[\{Ru(LL_n)\}_3Fe]^{8+}$ complexes appears as a single exponential with a luminescence lifetime slightly lower than those of the monometallic $[Ru(LL_n)]^{2+}$ complexes. Further experiments were performed on a subnanosecond timescale using a picosecond Ti:Sapphire laser and single photon counting detection. No additive short component in the decay was observed. Nevertheless, if the luminescence is detected, it is largely quenched. Indeed, compared to the $[Ru(LL_n)]^{2+}$ complexes, the luminescence quantum yield is lowered from a factor of 6 for $[\{Ru(LL_6)\}_3Fe]^{8+}$ to almost 10 for $[\{Ru(LL_4)\}_3Fe]^{8+}$ (Table 4). These data indicate that, as observed for $[Ru(LL_n)Fe]^{4+}$, the Fe^{II}-tris-bipyridine unit quenches the ^3MLCT excited state in the $[\{Ru(LL_n)\}_3Fe]^{8+}$ complexes.

The luminescence lifetime and quantum yield of the $[\{Ru(LL_n)\}_3Fe]^{8+}$ complexes were found to be independent of the concentration of the samples (concentration range used from 10^{-6} to 2×10^{-5} M), which means that, in contrast to what we demonstrated for the binuclear $[Ru(LL_n)Fe]^{4+}$ complexes, the intermolecular quenching is not efficient in such tetranuclear systems. As a result, the partial inhibition of the luminescence of the Ru^{II} centre is only due to an intramolecular interaction with the central Fe^{II}-tris-bipyridine unit.

Electron transfer (ET) between Ru^{II}* and Fe^{II} centres has to be ruled out for this quenching pathway. Indeed, considering the potential values of the $Ru^{II}*/Ru^{I}$ [in the range 0.34–0.38 V for $[\{Ru(LL_n)\}_3Fe]^{8+}$ vs. Ag/Ag^+ in CH_3CN with 0.1 M Bu_4NClO_4][18] and Fe^{II}/Fe^{III} (in the range 0.58–0.60 V) redox couples, the electron-transfer quenching process is strongly endergonic (≥0.2 V). Likewise, the potential value of the $Ru^{II}*/Ru^{III}$ redox couple (between –1.12 and –1.14 V) compared to that of the first reduction potential of the iron unit (between –1.647 and –1.687) leads to a strongly endergonic process (≥0.52 V). Thus, a pure electronic energy transfer (EET) can be considered as the main quenching process.[14,19]

The quenching rate constant (k_q) was determined from Equation (3), where φ_L^{Ref} and φ_L^{S} are the luminescence quantum yields of the $[Ru(LL_n)]^{2+}$ and $[\{Ru(LL_n)\}_3Fe]^{8+}$ complexes, respectively, and τ^{Ref} the luminescence lifetime of $[Ru(LL_n)]^{2+}$.

Table 4. Photophysical data determined for deoxygenated solutions of the ruthenium complexes in CH_3CN + 0.1 M Bu_4NClO_4 at 25 °C.

Complexes	λ_{emis} [nm]	τ [μs]	φ_L	k_q[a]	Ref.
$[Ru^{II}(bpy)_3]^{3+}$	603	1.06	0.062	9.0×10^9 $M^{-1}s^{-1}$[b]	[14,29]
$[Ru^{II}(LL_2)]^{2+}$	611	1.11	0.060	1.4×10^{10} $M^{-1}s^{-1}$[b]	[14]
$[Ru^{II}(LL_4)]^{2+}$	612	1.12	0.054	1.8×10^{10} $M^{-1}s^{-1}$[b]	[14]
$[Ru^{II}(LL_6)]^{2+}$	612	1.13	0.059	1.8×10^{10} $M^{-1}s^{-1}$[b]	[14]
$[Ru^{II}(LL_2)Fe^{II}]^{4+}$	612	1.10[c]	0.022[c]	3.5×10^8 $M^{-1}s^{-1}$	[14]
$[Ru^{II}(LL_4)Fe^{II}]^{4+}$	612	1.03[c]	0.019[c]	2.2×10^9 $M^{-1}s^{-1}$	[14]
$[Ru^{II}(LL_6)Fe^{II}]^{4+}$	612	1.00[c]	0.023[c]	3.3×10^9 $M^{-1}s^{-1}$	[14]
$[\{Ru^{II}(LL_2)\}_3Fe^{II}]^{8+}$	612	1.07	0.008	5.9×10^6 s^{-1}	this work
$[\{Ru^{II}(LL_4)\}_3Fe^{II}]^{8+}$	612	1.03	0.005	8.8×10^6 s^{-1}	this work
$[\{Ru^{II}(LL_6)\}_3Fe^{II}]^{8+}$	612	1.04	0.009	4.9×10^6 s^{-1}	this work
$[\{Ru^{II}(LL_2)]_3Zn^{II}\}^{8+}$	–	1.07	0.06	–	this work

[a] Quenching rate constant of the electronic energy transfer (EET) between Ru^{II}* and Fe^{II}. [b] Values determined in the presence of $[Fe(bpy)_3]^{2+}$. [c] Values determined for a 0.04 mM solution of binuclear complexes.

$$k_q = \left(\frac{\phi_L^{Ref}}{\phi_L^{S}} - 1\right) \times \frac{1}{\tau^{Ref}} \quad (3)$$

The same order of magnitude of k_q ($5\times10^6 \leq k_q \leq 9\times10^6$ s^{-1}; Table 4) was obtained for all three compounds, which shows that the EET process is moderately efficient and clearly not connected to the length to the aliphatic chain of the bridging ligand. Eliott and co-workers[15] have obtained a similar magnitude of k_q ($8\times10^6 \leq k_q \leq 197\times10^6$ s^{-1}) in aqueous methanolic solution, but, in contrast to our results, these authors found a dependence of the k_q value with the distance beween Ru^{II} and Fe^{II}: the more important the Ru^{II}–Fe^{II} distance, the weaker the k_q value. One can suggest that the nature of the solvent might have an influence on the deactivation process. This influence of solvation conditions is confirmed by the lower τ values obtained in aqueous methanolic medium for the precursor ruthenium complexes {τ = 356 ns for $[Ru(LL_2)]^{2+}$}.[15]

EET processes occur according to two mechanisms − Dexter (or electron exchange interaction)[20] and Förster (or coulombic interaction)[21] − both of which involve the spectral overlap of the luminescence of the donor with the absorption spectra of the acceptor. The Dexter mechanism requires contact between the donor and the acceptor, whereas the Förster one proceeds over a larger distance. For the Förster process, a critical transfer distance, R_0, can be calculated according to Equation (4)

$$R_0 = 1.25\times10^{17} \frac{\phi_D}{n^4} \int_0^\infty F_D(\bar{\nu})\varepsilon_A(\bar{\nu})\frac{d(\bar{\nu})}{\bar{\nu}^4} \quad (4)$$

where φ_D is the donor emission quantum yield {i.e. $[Ru(LL_n)]^{2+}$}, n the solvent refractive index and the integral term represents the spectral overlap of the normalised donor emission with the acceptor absorption. For the three $[\{Ru(LL_n)\}_3Fe]^{8+}$ complexes, an R_0 value of 20 ± 1 Å has been calculated, whereas the distance between the ruthenium and iron centres in theses structures is in the range from 10 to 12 Å according to space-filling molecular models.[15] When the estimated distance between both metallic centres is less than R_0, energy transfer is faster than radiative and non-radiative relaxation of the donor. Nevertheless, the fact that τ does not exhibit a systematic dependence on the Ru–Fe distance in the $[\{Ru(LL_n)\}_3Fe]^{8+}$ series suggests that the Förster mechanism should be considered as minor. Thus, the deactivation mainly proceeds by the Dexter mechanism. Therefore, since it involves the contact between the acceptor and the donor, the folding up of the molecule is required. Taking into account that the length of the alkyl chain does not lead to an important variation in τ, and that the deactivation process is mainly intramolecular, the experimental luminescence data can be understood if one considers that the tetranuclear complexes coexist in at least two forms in a thermodynamic equilibrium after irradiation in the MLCT band of the $[Ru(LL_n)]^{2+}$ subunit (Scheme 3). At the ground state level, the more stable geometry of the complexes is presumably the one which presents the four cationic metallic centres sufficiently distant to minimize the electrostatic repulsion. Quickly after the laser pulse irradiation, at the excited state level, the complexes undergo a sub-nanosecond (less than 30 ps) rearrangement, which cannot be detected by our setup, into two forms A and B (Scheme 3). In the A form, the relatively important Ru^{II}/Fe^{II} distance does not allow an efficient energy transfer (via a Dexter mechanism) and the luminescence of the ruthenium centre is detected with almost no perturbation due to the presence of the iron centre. It is well-known that, after irradiation in the MLCT band of the $[Ru(LL_n)]^{2+}$ moieties, an electron from the HOMO, which is localised around the metallic centre, is injected into the LUMO, which is delocalised over the bipyridine ligand, to form the transient $bpy^{\cdot-}$ radical anion.[22,23] In the B form, the two linked cationic metallic centres fold up in a way that confines the $bpy^{\cdot-}$ radical. Because two metallic centres are close, an efficient intramolecular EET is now feasible and contributes to the extinction of the luminescence of the complexes. From the luminescence quantum yield measurements, it appears that the B form is the more stable one at room temperature since φ_L decreases drastically from a factor of between 6 and 10 compared to that of $[Ru(LL_n)]^{2+}$ (Table 4). Moreover, if the A form and the B form are in rapid equilibrium, the excited state lifetime of the tetranuclear samples would be shorter than the corresponding

$[Ru(LL_n)]^{2+}$ as the relaxation channel for the B form is much faster than for the A form.[24] This effect is weak for $[\{Ru(LL_2)\}_3Fe]^{8+}$ {τ = 1.07 μs compared to 1.11 μs for $[Ru(LL_2)]^{2+}$} and larger for complexes having a longer aliphatic bridge such as n = 4 and n = 6 (Table 4).

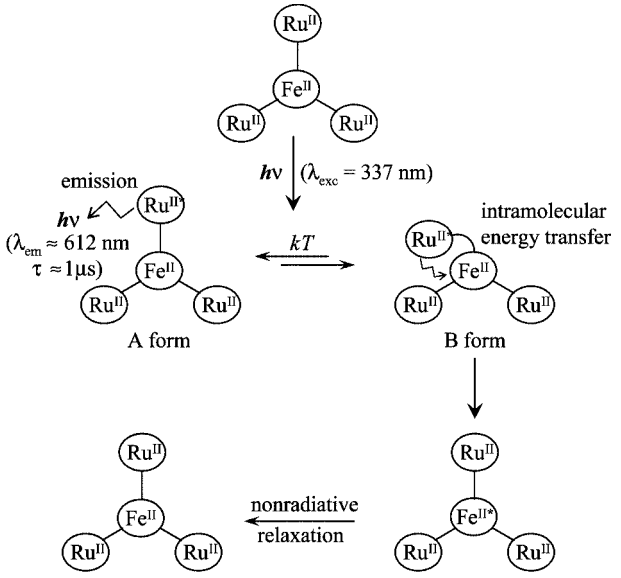

Scheme 3. Illustration of the photophysical behaviour of $[\{Ru(LL_n)\}_3Fe]^{8+}$ in CH_3CN + 0.1 M Bu_4NClO_4 after irradiation at 337 nm.

Although this phenomenon involves the proximity of cationic species, and therefore electrostatic repulsion, such an EET mechanism has already been suspected for other systems containing a $[Ru(bpy)_3]^{2+}$*-like donor with cationic iron[14,15] or manganese[12,25] complexes as acceptor. Nevertheless, the luminescence quantum yield of the $[\{Ru(LL_n)\}_3Fe]^{8+}$ complexes is much lower than that of $[Ru(LL_n)Fe]^{4+}$. To understand the reason for this difference, and to investigate the possibility of a self-quenching phenomenon of the Ru^{II}-tris-bipyridine units in the tetranuclear structure, we synthesised a similar tetranuclear complex in which Fe^{2+} is replaced by Zn^{2+}, namely $[\{Ru^{II}(bpy)_2(LL_2)\}_3Zn^{II}]^{8+}$ {denoted $[\{Ru(LL_2)\}_3Zn]^{8+}$}. The Zn^{II}-tris-bipyridine centre has no absorption in the visible region and, as expected, the absorption spectrum of the $[\{Ru(LL_2)\}_3Zn]^{8+}$ complex is close to that of $[Ru(LL_2)]^{2+}$. That excludes any possibility of an energy transfer between the Ru^{II}-tris-bipyridine units and the Zn^{II}-tris-bipyridine one after light irradiation. Moreover, since the Zn^{2+} site is not able to be oxidized, a quenching of the Ru^{II}* luminescence by an electron transfer is thermodynamically prohibited. The quantum yield and luminescence lifetime of $[\{Ru(LL_2)\}_3Zn]^{8+}$ were determined to be φ_L = 0.06 and τ = 1.07 μs, respectively. These values are similar to those obtained for $[Ru(LL_2)]^{2+}$ (φ_L = 0.06, τ = 1.11 μs), only the lifetime is weakly decreased as for $[\{Ru(LL_2)\}_3Fe]^{8+}$, indicating that the possible self-quenching of the similar $[Ru(LL_2)]^{2+}$ centre has to be considered as a minor process. Thus, the drastically lowered φ_L value for the $[\{Ru(LL_n)\}_3Fe]^{8+}$ complexes compared to $[Ru(LL_n)Fe]^{4+}$ can only be due to a higher probability of a dynamic quenching between Fe and Ru by folding up of the molecule in the tetranuclear structures than in the binuclear ones.

Photoinduced Electron Transfer

It has been established previously[14,26,27] that addition of an irreversible electron acceptor like 4-bromophenyldiazonium tetrafluoroborate ($ArN_2^+BF_4^-$) to a solution of the $[Ru^{II}(bpy)_3]^{2+}$ complex in CH_3CN + 0.1 M Bu_4NClO_4 allows the efficient production of $[Ru^{III}(bpy)_3]^{3+}$ under continuous irradiation (quantum yield 0.34). This permanent build up of $[Ru^{III}(bpy)_3]^{3+}$ arises because of the following electron transfer quenching reaction [Equations (5) and (6)]; the back-electron transfer reaction between $[Ru^{III}(bpy)_3]^{3+}$ and $ArN_2^{\cdot}$ radical is avoided by the rapid evolution of $ArN_2^{\cdot}$ into ArH and N_2.[25,26]

$$[Ru^{II}(bpy)_3]^{2+}* + ArN_2^+ \rightarrow [Ru^{III}(bpy)_3]^{3+} + ArN_2^{\cdot} \quad (5)$$

$$ArN_2^{\cdot} \xrightarrow{CH_3CN} ArH + N_2 \quad (6)$$

In the binuclear $[Ru(LL_n)Fe]^{4+}$ complexes, it has been demonstrated that ArN_2^+ can also react preferentially with the excited state of the $[Ru(LL_n)]^{2+}$ subunit to advantageously short-circuit the energy transfer.[14] For tetranuclear complexes, a similarly efficient photogeneration of the corresponding Ru^{III} species, i.e. $[Ru^{III}Ru^{II}_2(bpy)_6(LL_n)_3Fe^{II}]^{9+}$ is expected (Scheme 2). Indeed, the quenching of the Ru^{II}* centre in the $[\{Ru(LL_n)\}_3Fe]^{8+}$ complexes by EET is incomplete and the luminescence lifetime of the Ru^{II}* excited state is sufficiently long-lived (1 μs) to allow a bimolecular reaction using an external electron acceptor. In addition, the lifetime of the excited state of the Fe^{II} moiety is too short (<1 ns) to undergo an efficient bimolecular electron transfer with ArN_2^+.[19]

In order to photoinduce the oxidation of the $[\{Ru(LL_n)\}_3Fe]^{8+}$ complexes, ArN_2^+ was added to a solution of the complexes in deoxygenated CH_3CN + 0.1 M Bu_4NClO_4. Since the photogenerated Ru^{III} subunit plays the role of oxidant towards Fe^{II} (see electrochemical part), irradiation should lead, in a first step, to $[\{Ru^{II}(LL_n)\}_3Fe^{III}]^{9+}$ (Scheme 2). In a second step, the formation of the final $[\{Ru^{III}(LL_n)\}_3Fe^{III}]^{12+}$ species is expected as ArN_2^+ is added in excess. The rate constant of oxidant quenching (k_{ET}) of the excited state of the tetranuclear complexes by ArN_2^+ was determined from the Stern–Volmer plot, see Equation (7)

$$\tau/\tau_{Ar} = 1 + k_{ET}\cdot\tau\cdot[ArN_2^+] \quad (7)$$

where τ and τ_{Ar} are the luminescence lifetime of the complexes without and with a variable concentration of ArN_2^+, respectively, and k_{ET} is the rate constant of the electron transfer reaction according to Equation (8).

$$[Ru^{II}*Ru^{II}_2(bpy)_6(LL_n)_3Fe^{II}]^{8+} + ArN_2^+ \xrightarrow{k_{ET}} [Ru^{III}Ru^{II}_2(bpy)_6(LL_n)_3Fe^{II}]^{9+} + ArN_2^{\cdot} \quad (8)$$

The Stern–Volmer plots are linear for the three complexes (Figure 5). This indicates that the electron transfer is a simple bimolecular reaction, i.e. only one Ru^{II} centre reacts each time with ArN_2^+. The k_{ET} values obtained for the tetranuclear $[\{Ru(LL_n)\}_3Fe]^{8+}$ compounds ($>10^9$ $M^{-1}s^{-1}$) depend only slightly on the Ru–Fe distance in the complexes, and are around 10 times greater than the k_{ET} values determined for the binuclear $[Ru(LL_n)Fe]^{4+}$ complexes (Table 5). The markedly faster electronic quenching process in the case of tetranuclear complexes is presumably due to the lower efficiency of the competitive energy transfer by the Fe^{2+} centre (Table 4). Nevertheless, it is difficult to compare the energy-transfer constants of these two kinds of complexes since, for the tetranuclear complexes, the energy transfer occurs via an intramolecular process while for the binuclear ones it is intermolecular.

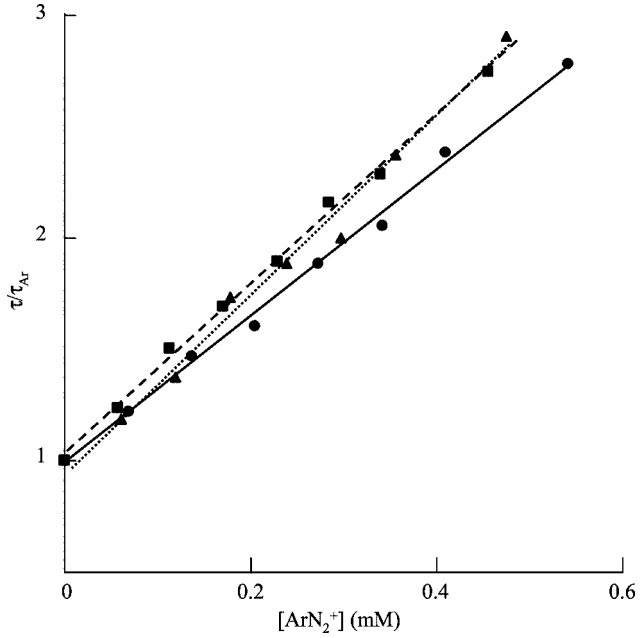

Figure 5. Stern–Volmer plots for the $[\{Ru(LL_n)\}_3Fe]^{8+}$ complexes in deoxygenated CH_3CN (0.01 mM) with ArN_2^+ (between 0 and 0.6 mM): $[\{Ru(LL_2)\}_3Fe]^{8+}$ (■), $[\{Ru(LL_4)\}_3Fe]^{8+}$ (●) and $[\{Ru(LL_6)\}_3Fe]^{8+}$ (▲).

Table 5. Electron transfer rate constant, k_{ET}, for $[Ru(LL_n)Fe]^{4+}$ and $[\{Ru(LL_n)\}_3Fe]^{8+}$ in the presence of a variable concentration of ArN_2^+ at room temperature in CH_3CN + 0.1 M Bu_4NClO_4.

Complexes	k_{ET} [$M^{-1}s^{-1}$]
$[Ru^{II}(LL_2)Fe^{II}]^{4+}$	3.7×10^8
$[Ru^{II}(LL_4)Fe^{II}]^{4+}$	5.3×10^8
$[Ru^{II}(LL_6)Fe^{II}]^{4+}$	6.4×10^8
$[\{Ru^{II}(LL_2)\}_3Fe^{II}]^{8+}$	3.6×10^9
$[\{Ru^{II}(LL_4)\}_3Fe^{II}]^{8+}$	3.2×10^9
$[\{Ru^{II}(LL_6)\}_3Fe^{II}]^{8+}$	4.0×10^9

Photooxidation by Continuous Irradiation

Successive photogeneration of the oxidized $[\{Ru^{II}(LL_n)\}_3Fe^{III}]^{9+}$ and $[\{Ru^{III}(LL_n)\}_3Fe^{III}]^{12+}$ species (Scheme 2) was followed by UV/Vis absorption spectroscopy. Solutions containing $[\{Ru(LL_n)\}_3Fe]^{8+}$ (0.03–0.04 mM) in the presence of an excess of ArN_2^+ (15 mM) in CH_3CN + 0.1 M Bu_4NClO_4 were irradiated with a mercury lamp (250 W). Two successive changes of the absorption spectrum were observed during the irradiation. In the first step, the band of the Fe^{II} unit at 530 nm decreases regularly until it disappears totally, in accordance with the formation of $[\{Ru^{II}(LL_n)\}_3Fe^{III}]^{9+}$ via the transient photogenerated Ru^{III} species (Figure 6). In a second step, irradiation induces the quantitative formation of $[\{Ru^{III}(LL_n)\}_3Fe^{III}]^{12+}$, as illustrated by the decrease of the MLCT band of the Ru^{II} unit at around 455 nm and the appearance of two new ones at 428 and 644 nm typical of the Ru^{III} species.

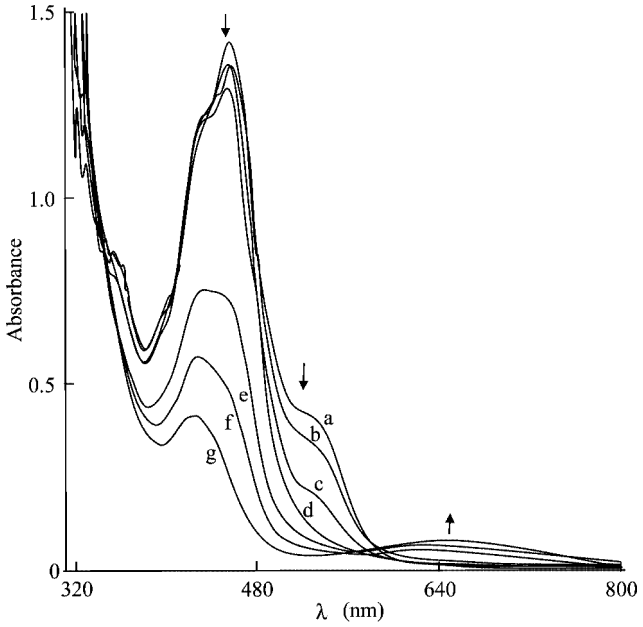

Figure 6. Spectral change of a mixture of $[\{Ru(LL_6)\}_3Fe]^{8+}$ (0.032 mM) and ArN_2^+ (15 mM), under visible irradiation: (a) initial solution, (b) 3 s, (c) 12 s, (d) 24 s, (e) 120 s, (f) 220 s, (g) 700 s, (l = 1 cm).

From a kinetic point of view, one can consider that, during the first step, there is a steady-state concentration of the Ru^{II} and Ru^{III} species since the sacrificial oxidant is present in large excess. Thus, the overall kinetic law for the oxidation of the Fe^{II}-tris-bipyridine unit can, as we previously proposed,[14] be approximated to a pseudo-first-order equation [Equation (9)], where $[Ru^{II}]$ and $[Fe^{II}]$ represent the concentration of the two subunits of the $[\{Ru(LL_n)\}_3Fe]^{8+}$ complexes in solution.

$$v = k[Ru^{II}][Fe^{II}][ArN_2^+] = K_{Fe}[Fe^{II}] = -d[Fe^{II}]/dt \quad (9)$$

In a similar fashion, during the second step involving the formation of $[\{Ru^{III}(LL_n)\}_3Fe^{III}]^{12+}$, a pseudo-first-order equation is also obtained, see Equation (10).

Table 6. Apparent oxidation rate constants for $[\{Ru(LL_n)\}_3Fe]^{8+}$ during irradiation in the presence of a large excess of ArN_2^+.

Complexes	K_{Fe} [s^{-1}]	K_{Ru} [s^{-1}]
$[\{Ru^{II}(LL_2)\}_3Fe^{II}]^{8+}$	$5.4\times10^{-2}\pm0.8\times10^{-2}$	$4.99\times10^{-3}\pm4\times10^{-5}$
$[\{Ru^{II}(LL_4)\}_3Fe^{II}]^{8+}$	$8.4\times10^{-2}\pm0.6\times10^{-2}$	$6.63\times10^{-3}\pm6\times10^{-5}$
$[\{Ru^{II}(LL_6)\}_3Fe^{II}]^{8+}$	$11.7\times10^{-2}\pm1\times10^{-2}$	$12.24\times10^{-3}\pm3\times10^{-5}$

$$v = k'[Ru^{II}][Fe^{III}][ArN_2^+] = K_{Ru}[Ru^{II}] = -d[Ru^{II}]/dt \quad (10)$$

These two oxidation steps were followed by the evolution of the absorbance at 530 and 454 nm, respectively, with the irradiation time. In all cases the absorbance variation was fitted by a monoexponential curve, as illustrated in Figure 7, in accordance with Equations (9) and (10), thus allowing the determination of K_{Fe} and K_{Ru} for the three heterotetranuclear complexes. These values are given in Table 6. It appears that both the Fe^{II} and Ru^{II} oxidation rate depend on the nature of the bridging ligand, and that the efficiency of the photoassisted process increases when the length of the alkyl chain increases, oxidation of $[\{Ru(LL_6)\}_3Fe]^{8+}$ being twice as fast as oxidation of $[\{Ru(LL_2)\}_3Fe]^{8+}$.

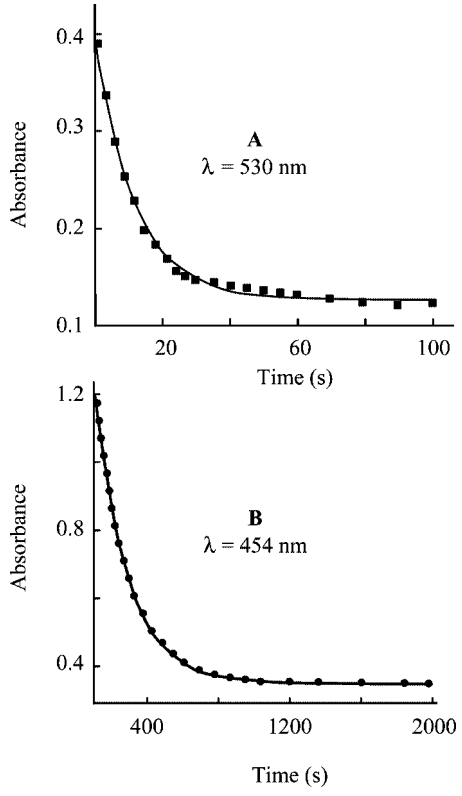

Figure 7. Evolution of the absorption intensity at 530 nm (A) and 454 nm (B) with irradiation time for the $[\{Ru(LL_6)\}_3Fe]^{8+}$ complexes (0.032 mM) in CH_3CN + 0.1 M Bu_4NClO_4, in the presence of ArN_2^+ (15 mM) (l = 1 cm). Bold lines correspond to the fit using a monoexponetial function. The fit parameters K_{Fe} and K_{Ru} are given in Table 6.

Two processes can control the overall efficiency of the oxidation steps and explain the influence of the aliphatic chain length on the photooxidation rate. The first one is the photogeneration of the Ru^{III} moieties. This process requires contact between two cationic species {i.e. ArN_2^+ and $[\{Ru(LL_n)\}_3Fe]^{8+}$} and involves an electrostatic repulsion phenomenon which should be important for the complex exhibiting the smaller Ru–Fe distance − $[\{Ru(LL_2)\}_3Fe]^{8+}$ − whereas it is less pronounced for $[\{Ru(LL_6)\}_3Fe]^{8+}$. The second process involves the oxidation of Fe^{II} into Fe^{III}. Since the electron transfer operates according to an intramolecular process, it requires the folding-up of the complex in order to allow the formation of Fe^{III} through the photogenerated Ru^{III} moieties. Taking into account that the flexibility of the aliphatic bridging ligand increases with the number of methylene units, the contact between Ru^{III} and Fe^{II} should be favoured in the case of $[\{Ru(LL_6)\}_3Fe]^{8+}$, whereas for $[\{Ru(LL_2)\}_3Fe]^{8+}$ the folding-up is more difficult and therefore the photooxidation rate is lowered.

Finally, the quantum yield of formation of $[\{Ru^{II}(LL_n)\}_3Fe^{III}]^{9+}$ (φ_F) was determined in CH_3CN (see Experimental Section) and was found to be equal to 0.22 for the most efficient system, i.e. $[\{Ru(LL_6)\}_3Fe]^{8+}$.

Conclusions

In this study we have demonstrated that for the tetranuclear $[\{Ru^{II}(LL_n)\}_3Fe^{II}]^{8+}$ complexes a partial energy transfer from the ^{3}MLCT excited state of the Ru^{II}-tris-bipyridine centres to the Fe^{II}-tris-bipyridine unit occurs by a pure intramolecular process, in contrast to what was observed for the corresponding binuclear complexes. This is a consequence of the structure of the tetranuclear complexes, in which the presence of the three Ru^{II} subunits prevents the close contact of the Fe^{II} centre with the Ru^{II} subunits of another tetranuclear complex and therefore an intermolecular energy transfer. The rate constant of the process is not clearly connected to the length of the aliphatic chain of the bridging ligand. This energy-transfer process can be easily short-circuited in the presence of an external irreversible electron acceptor by an electron-transfer process, leading, with a high quantum yield, to the photoinduced oxidation of the iron(II) subunit of the tetranuclear complexes (φ_F = 0.22) followed by that of the ruthenium(II) subunits.

An extension of this work is currently underway with similar tetranuclear polypyridyl complexes of Ru^{II} and Mn^{II}. An efficient photoinduced oxidation phenomenon is also expected for this kind of complex since the energy transfer between the two different metallic subunits is known to be less efficient than for the parent Fe^{II} compounds.

Experimental Section

General: Acetonitrile (Rathburn, HPLC grade) was used as received and stored under argon in a glovebox. Tetra-*n*-butylammonium perchlorate (Bu_4NClO_4, Fluka) was used as received. ^1H NMR spectra were recorded on a Bruker AC 250 spectrometer. The electrospray ionisation mass spectrometry (ESI-MS) experiments were performed on a triple quadrupole mass spectrometer Quattro II (micromass, Altrincham, UK). The ESI source was heated to 80 °C. The sampling cone voltage was set within the range 6–17 V according to the complex studied. Complexes in solution (1 mg mL^{-1} in CH_3CN) were injected using a syringe pump at a flow rate of 10 μL min^{-1}. The electrospray probe (capillary) voltage was optimised in the range 2–5 kV for positive ion electrospray. Elemental analyses were performed by the Service Central d'Analyse du CNRS at Vernaison (France). UV/Vis spectra were obtained using a Cary 1 and a Cary 100 absorption spectrophotometers on 1-mm path-length quartz cells for electrochemical experiments and 1-cm cells for irradiation experiments.

Electrochemistry: All electrochemical measurements were performed under argon in a glovebox at room temperature. Cyclic voltammetry and controlled potential electrolysis experiments were performed using an EG&G PAR model 173 potentiostat/galvanostat equipped with a PAR model universal programmer and a PAR model 179 digital coulometer. A CHI440 Electrochemical Analyzer (CH Instruments, Texas, USA) was used for the determination of formal potentials. A standard three-electrode electrochemical cell was used. Potentials were referenced to an Ag/10 mM $AgNO_3$ reference electrode in CH_3CN + 0.1 M Bu_4NClO_4. Potentials referred to that system can be converted into the ferrocene/ferrocenium couple by subtracting 87 mV and to SCE or NHE by adding 298 mV or 548 mV, respectively.[28] The working electrode was a platinum disk polished with 2-μm diamond paste (Mecaprex Presi) with a diameter of 5 mm for cyclic voltammetry [E_{pa}: anodic peak potential; E_{pc}: cathodic peak potential; $E_{1/2} = (E_{pa} + E_{pc})/2$; $\Delta E_p = E_{pa} - E_{pc}$] and 2 mm for rotating disk electrode experiments (RDE). Exhaustive electrolyses were carried out with a platinum plate. The auxiliary electrode was a Pt wire in CH_3CN + 0.1 M Bu_4NClO_4. For electrochemical experiments, electronic absorption spectra were recorded on a Hewlett–Packard 8452 A diode array spectrophotometer. Initial and electrolyzed solutions were transferred to a conventional 1-mm quartz cell in the glovebox.

Luminescence: The steady-state emission spectra were recorded on a Photon Technology International (PTI) SE-900M spectrofluorimeter. All the samples for luminescence and photooxidation experiments were prepared in a glovebox in deoxygenated CH_3CN + 0.1 M Bu_4NClO_4 and contained in a 1-cm quartz cell. The samples were maintained under aerobic conditions with a Teflon cap. The luminescence lifetime of the complexes was recorded after irradiation at λ = 337 nm with a 4-ns pulsed laser (spectra physics 337-201) and recorded at λ = 600 nm using a monochromator and a photomultiplicator tube (Hammamatsu R928) coupled with an ultra-fast oscilloscope (Tektronix TDS 520A). For subnanosecond decay experiments, sample excitation was performed at 400 nm, which was obtained by the second harmonic of a Titanium: Sapphire laser (picosecond Tsunami laser at an 80-MHz repetition rate). For decay acquisition, a GaAs microchannel plate photomultiplier (Hamamatsu model R 3809 U-51) followed by a homemade single-photon correlator were used. The ultimate time resolution of the entire chain was close to 30 ps. The emission quantum yield, φ_L, was determined at 25 °C in deoxygenated acetonitrile solutions with a CH_3CN solution of $[Ru^{II}(bpy)_3](PF_6)_2$ ($\varphi_L^{ref} = 0.062$)[29] according to Equation (11)

$$\phi_L^S = \frac{I_L^S}{I_L^{Ref}} \frac{(1-10^{-OD^{Ref}})}{(1-10^{-OD^S})} \phi_L^{Ref} \quad (11)$$

where the emission intensity, I_L, was calculated from the spectrum area $\int I(\lambda)d\lambda$, and OD represents the optical density at the excitation wavelength (450 nm). The superscripts "S" and "Ref" refer to the sample and to the standard, respectively.

Continuous Irradiation: The irradiation experiments were performed using a mercury lamp (Oriel 66901, 250 W) whose UV and IR radiations were filtered with a large band-pass filter centred around λ = 560 nm (irradiation range between 410 and 710 nm). The solutions contained a mixture of $[\{Ru(LL_n)\}_3Fe]^{8+}$ complex (0.03–0.04 mM) and ArN_2^+ (15 mM) in order to obtain an absorbance below 1.5 at 454 nm in CH_3CN + 0.1 M Bu_4NClO_4. Under these conditions the concentration of ArN_2^+ can be considered as constant during the experiments.

The quantum yields of formation of $[\{Ru^{II}(LL_n)\}_3Fe^{III}]^{9+}$, φ_F, measured after continuous irradiation at 436 nm, were performed with a 250-W Hg Lamp (Oriel 66901). The desired mercury emission line was isolated using a band-pass filter. The quantum yields were determined by actinometry at the wavelength of the maximum absorption of $[Fe(bpy)_3]^{2+}$ (526 nm) by comparing the absorption of the sample before and after irradiation and using the quantum yield formation of $[Ru(bpy)_3]^{3+}$ in the system $[Ru(bpy)_3]^{2+}/ArN_2^+$ as reference ($\varphi_F^{Ref} = 0.34$).[26] Samples were prepared with the same absorbance (Abs = 2) at 454 nm and the variation of absorbance during irradiation was checked to be less than 0.1. The quantum yield of formation, φ_F^S, of the sample was deduced from Equation (12).

$$\phi_F^S = \left[\frac{(\Delta OD)^S_{526\,nm}}{(\Delta OD)^{Ref}_{454\,nm}}\right]_{t,\lambda^{irr}=436\,nm} \times \phi_F^{Ref} \quad (12)$$

Synthesis of the Diazonium Salt: 4-bromophenyl diazonium tetrafluoroborate *p*-$BrC_6H_4N_2^+ \cdot BF_4^-$ ($ArN_2^+ \cdot BF_4^-$) was synthesised as described previously.[26]

Synthesis of Ligands LL_n and of $[Ru^{II}(bpy)_2(LL_n)](PF_6)_2$: The ligands 1,2-bis[4-(4′-methyl-2,2′-bipyridinyl)]ethane (LL_2), 1,2-bis[4-(4′-methyl-2,2′-bipyridinyl)]butane (LL_4), 1,2-bis[4-(4′-methyl-2,2′-bipyridinyl)]hexane (LL_6) and the $[Ru^{II}(bpy)_2(LL_2)](PF_6)_2$, $[Ru^{II}(bpy)_2(LL_4)](PF_6)_2$, $[Ru^{II}(bpy)_2(LL_6)](PF_6)_2$ complexes were synthesised as described previously.[14]

Synthesis of $[\{Ru^{II}(bpy)_2(LL_n)\}_3Fe^{II}](PF_6)_8$: An aqueous solution of 0.4 molar equivalents of $Fe(ClO_4)_2 \cdot 8H_2O$ was added to an orange solution of $[Ru^{II}(bpy)_2(LL_n)](PF_6)_2$ (100 mg) in ethanol (10 mL) at 60 °C, leading to the formation of the red-orange complex $[\{Ru^{II}(bpy)_2(LL_n)\}_3Fe^{II}]^{8+}$. After stirring the solution for one hour at 60 °C, the ethanol was removed under reduced pressure and the heterotetranuclear complex was extracted with CH_2Cl_2. The resulting solution was washed three times with an aqueous KPF_6 solution (0.1 M) in order to exchange the ClO_4^- anion with PF_6^-, and then twice with water. After drying over Na_2SO_4, CH_2Cl_2 was removed under reduced pressure. The red-orange product obtained corresponding to $[\{Ru^{II}(bpy)_2(LL_n)\}_3Fe^{II}](PF_6)_8$ was reprecipitated in CH_3CN/diethyl ether, washed with diethyl ether, and dried under vacuum. The purity of each complex was confirmed by elemental analysis, ^1H NMR spectroscopy and by the observation of a single spot by TLC [eluent H_2O/CH_3CN (10:90) containing KPF_6 (10 mM)].

$[\{Ru^{II}(bpy)_2(LL_2)\}_3Fe^{II}](PF_6)_8$ ($[\{Ru(LL_2)\}_3Fe]^{8+}$): 51 mg (45%). $C_{132}H_{114}F_{48}Fe_1N_{24}P_8Ru_3{\cdot}6H_2O$ (3663.3): calcd. C 43.28, H 3.46, N 9.18; found C 43.42, H 3.33, N 9.36. ESI-MS: *m/z* (%) = 3410.28 $[M - PF_6]^+$, 1632.70 (2) $[M - 2PF_6]^{2+}$, 1040.15 (6) $[M - 3PF_6]^{3+}$, 743.87 (10) $[M - 4PF_6]^{4+}$, 566.10 (42) $[M - 5PF_6]^{5+}$.

$[\{Ru^{II}(bpy)_2(LL_4)\}_3Fe^{II}](PF_6)_8$ ($[\{Ru(LL_4)\}_3Fe]^{8+}$): Yield: 46 mg (41%). $C_{138}H_{126}F_{48}Fe_1N_{24}P_8Ru_3{\cdot}6H_2O$ (3747.5): calcd. C 44.34, H 3.71, N 9.04; found C 44.82, H 3.72, N 9.03. ESI-MS: *m/z* (%): 3494.44 $[M - PF_6]^+$, 1674.75 (1) $[M - 2PF_6]^{2+}$, 1068.18 (8) $[M - 3PF_6]^{3+}$, 764.90 (17) $[M - 4PF_6]^{4+}$, 582.92 (53) $[M - 5PF_6]^{5+}$.

$[\{Ru^{II}(bpy)_2(LL_6)\}_3Fe^{II}](PF_6)_8$ ($[\{Ru(LL_6)\}_3Fe]^{8+}$): Yield: 24 mg (22%). $C_{144}H_{138}F_{48}Fe_1N_{24}P_8{\cdot}Ru_36H_2O$ (3831.65): calcd. C 45.14, H 3.94, N 8.78; found C 45.63, H 3.91, N 8.96. ESI-MS: *m/z* (%): 3578.60 $[M - PF_6]^+$, 1726.80 (1) $[M - 2PF_6]^{2+}$, 1096.22 (8) $[M - 3PF_6]^{3+}$, 785.92 (22) $[M - 4PF_6]^{4+}$, 599.74 (59) $[M - 5PF_6]^{5+}$.

Synthesis of $Zn(CF_3SO_3)_2$: Pure CF_3SO_3H (1 mL, 11.2 mmol) was added to a solution of CH_3CN (10 mL) containing Zn powder (7.13 g, 112 mmol). After stirring for one day, the excess of Zn was removed by filtration. Addition of diethyl ether to the filtrate yielded the formation of a white precipitate of $Zn(CF_3SO_3)_2$, which was filtered off, washed with diethyl ether and dried under vacuum (yield: 1.02 g, 50%).

Synthesis of $[\{Ru^{II}(bpy)_2(LL_2)\}_3Zn^{II}](PF_6)_8$: Solid $Zn(CF_3SO_3)_2$ (2.36 mg, 6.48 μmol) was added to a solution of $[Ru^{II}(bpy)_2(LL_2)](PF_6)_2$ (20.8 mg, 19.4 μmol) in ethanol (80 mL), leading to the formation of the $[\{Ru^{II}(bpy)_2(LL_2)\}_3Zn^{II}\}^{8+}$ complex. This solution was stirred for one hour at reflux. After cooling to room temperature, an aqueous solution (20 mL) of KPF_6 (15 mg, 64.8 μmol) was added and then the ethanol was removed under reduced pressure. The heterotetranuclear complex was extracted from the aqueous phase with CH_2Cl_2. The resulting CH_2Cl_2 solution was washed three times with an aqueous KPF_6 solution (0.1 M), and then twice with water. After drying over Na_2SO_4, CH_2Cl_2 was removed under reduced pressure. The orange product obtained corresponding to $[\{Ru^{II}(bpy)_2(LL_2)\}_3Zn^{II}](PF_6)_8$ was reprecipitated from CH_3CN/diethyl ether, washed with diethyl ether, and dried under vacuum (yield: 18.5 mg, 80%). $C_{132}H_{114}F_{48}N_{24}Ru_3P_8Zn_1$ (3564.8): calcd. C 44.47, H 3.22, N 9.43; found C 44.49, H 3.29, N 9.60.

Acknowledgments

We thank Dr. Jean-Claude Vial from the Laboratoire de Spectrométrie Physique (CNRS UMR 5588, Université Joseph Fourier, Grenoble I) for allowing us to use his picosecond emission decay setup. We also thank one referee for pointing out that the kinetics of two excited states in rapid equilibrium were worked out thoroughly by J. N. Demas.

[1] M. R. Wasielewski, *Chem. Rev.* **1992**, *92*, 435.
[2] V. Balzani, A. Juris, M. Venturi, *Chem. Rev.* **1996**, *96*, 759.
[3] C. A. Bignozzi, J. R. Schoonover, F. Scandola, *Prog. Inorg. Chem.* **1997**, *44*, 1, special volume on molecular level artificial photosynthetic materials (Eds.: G. J. Meyer, K. D. Karlin), John Wiley & Sons, New York.
[4] L. Sun, L. Hammarström, B. Akermark, S. Styring, *Chem. Soc. Rev.* **2001**, *30*, 36.
[5] L. Hammarström, *Curr. Opin. Chem. Biol.* **2003**, *7*, 666.
[6] D. Burdinski, K. Wieghardt, S. Steenken, *J. Am. Chem. Soc.* **1999**, *30*, 10781.
[7] D. Burdinski, B. Eberhardt, K. Wieghardt, *Inorg. Chem.* **2000**, *39*, 105.
[8] K. E. Berg, A. Tran, M. K. Raymond, M. Abrahamsson, J. Wolny, S. Redon, M. Andersson, L. Sun, L. Hammarström, H. Toftlund, B. Akermark, *Eur. J. Inorg. Chem.* **2001**, 1019.
[9] M. M. Morrisson, D. T. Sawyer, *Inorg. Chem.* **1978**, *17*, 333.
[10] M. N. Collomb Dunand-Sautier, A. Deronzier, *J. Electroanal. Chem.* **1997**, *428*, 65.
[11] M. N. Collomb Dunand-Sautier, A. Deronzier, I. Romero, *J. Electroanal. Chem.* **1997**, *436*, 219.
[12] H. Berglund-Baudin, L. Sun, R. Davidov, M. Sundahl, S. Styring, B. Akermark, M. Almgren, L. Hammarström, *J. Phys. Chem. A* **1998**, *102*, 2512.
[13] M. Abrahamsson, H. Baudin, A. Tran, C. Philouze, K. E. Berg, M. K. Raymond-Johansson, L. Sun, B. Akermark, S. Styring, L. Hammarström, *Inorg. Chem.* **2002**, *41*, 1534.
[14] F. Lafolet, J. Chauvin, M.-N. Collomb, A. Deronzier, H. Laguitton-Pasquier, J.-C. Leprêtre, J.-C. Vial, B. Brasme, *Phys. Chem. Chem. Phys.* **2003**, *5*, 2520.
[15] R. H. Schmehl, R. A. Auerbach, W. F. Wacholtz, C. M. Elliott, R. A. Freitag, J. W. Merkert, *Inorg. Chem.* **1986**, *25*, 2440.
[16] A. E. Kaifer, M. Gomez-Kaifer, *Supramolecular Electrochemistry*, Chap. 8 "Electrochemical Considerations for Supramolecular Systems", Wiley-VCH Weinheim, Germany ,**1999**, p. 89.
[17] J. B. Flanagan, S. Margel, A. J. Bard, F. C. Anson, *J. Am. Chem. Soc.* **1977**, *100*, 4248.
[18] The potentials of the Ru^{II*}/Ru^{I} and Ru^{II*}/Ru^{III} redox couples were estimated by subtracting 2.03 eV (λ_{emis} = 612 nm) from the potential of Ru^{II}/Ru^{I} and Ru^{II}/Ru^{III} of the $[\{Ru(LL_n)\}_3Fe]^{8+}$ complexes.
[19] C. Creutz, M. Chou, T. Netzel, M. Okumura, N. Sutin, *J. Am. Chem. Soc.* **1980**, *102*, 1309.
[20] L. D. Dexter, *J. Chem. Phys.* **1953**, *21*, 838.
[21] T. H. Förster, *Discuss. Faraday Soc.* **1959**, *27*, 7.
[22] A. Juris, V. Balzani, F. Barrigelletti, S. Campagna, P. Belser, A. von Zelewsky, *Coord. Chem. Rev.* **1988**, *84*, 85–277.
[23] G. F. Strousse, J. R. Schoonover, R. Duesing, S. Boyde, W. E. Jones, T. J. Meyer, *Inorg. Chem.* **1995**, *34*, 473.
[24] J. N. Demas, *Excited State Lifetime Measurements*, Academic Press, New York, **1983**.
[25] C. Baffert, S. Dumas, J. Chauvin, J.-C. Leprêtre, M.-N. Collomb, A. Deronzier, *Phys. Chem. Chem. Phys.* **2005**, *7*, 202.
[26] H. Cano-Yelo, A. Deronzier, *J. Chem. Soc., Faraday Trans. 1* **1984**, *80*, 3011.
[27] H. Laguitton-Pasquier, A. Martre, A. Deronzier, *J. Phys. Chem. B* **2001**, *105*, 4801.
[28] V. V. Pavlishchuk, A. W. Addison, *Inorg. Chim. Acta* **2000**, *298*, 97.
[29] J. V. Caspar, T. J. Meyer, *J. Am. Chem. Soc.* **1983**, *105*, 5583.

Received: February 2, 2005
Published Online: July 7, 2005

